



■ CARTILAGE

CircStrn3 targeting *microRNA-9-5p* is involved in the regulation of cartilage degeneration and subchondral bone remodelling in osteoarthritis

**B. Li,
T. Ding,
H. Chen,
C. Li,
B. Chen,
X. Xu,
P. Huang,
F. Hu,
L. Guo**

From Shanghai Jiao
Tong University School
of Medicine, Shanghai,
China

Aims

Circular RNA (circRNA) is involved in the regulation of articular cartilage degeneration induced by inflammatory factors or oxidative stress. In a previous study, we found that the expression of *circStrn3* was significantly reduced in chondrocytes of osteoarthritis (OA) patients and OA mice. Therefore, the aim of this paper was to explore the role and mechanism of *circStrn3* in osteoarthritis.

Methods

Minus RNA sequencing, fluorescence in situ hybridization, and quantitative real-time polymerase chain reaction (qRT-PCR) were used to detect the expression of *circStrn3* in human and mouse OA cartilage tissues and chondrocytes. Chondrocytes were then stimulated to secrete exosomal miR-9-5p by cyclic tensile strain. Intra-articular injection of exosomal miR-9-5p into the model induced by destabilized medial meniscus (DMM) surgery was conducted to alleviate OA progression.

Results

Tensile strain could decrease the expression of *circStrn3* in chondrocytes. *CircStrn3* expression was significantly decreased in human and mouse OA cartilage tissues and chondrocytes. *CircStrn3* could inhibit matrix metabolism of chondrocytes through competitively 'sponging' miRNA-9-5p targeting Kruppel-like factor 5 (*KLF5*), indicating that the decrease in *circStrn3* might be a protective factor in mechanical instability-induced OA. The tensile strain stimulated chondrocytes to secrete exosomal miR-9-5p. Exosomes with high *miR-9-5p* expression from chondrocytes could inhibit osteoblast differentiation by targeting *KLF5*. Intra-articular injection of exosomal *miR-9-5p* alleviated the progression of OA induced by destabilized medial meniscus surgery in mice.

Conclusion

Taken together, these results demonstrate that reduction of *circStrn3* causes an increase in *miR-9-5p*, which acts as a protective factor in mechanical instability-induced OA, and provides a novel mechanism of communication among joint components and a potential application for the treatment of OA.

Cite this article: *Bone Joint Res* 2023;12(1):33–45.

Keywords: Osteoarthritis, *CircStrn3*, *microRNA-9-5p*, Kruppel-like factor 5, Exosome

Article focus

■ *CircStrn3* could inhibit matrix metabolism of chondrocytes through competitively 'sponging' miRNA-9-5p targeting Kruppel-like factor 5 (*KLF5*).

Key messages

■ Intra-articular injection of exosomal *miR-9-5p* alleviates the progression of osteoarthritis (OA) in mice.

Correspondence should be sent to
Lei Guo; email:
guolei_sjt@126.com; hfq_sjt@
126.com

doi: 10.1302/2046-3758.121.BJR-
2022-0231.R1

Bone Joint Res 2023;12(1):33–45.

- Exosomes with high *miR-9-5p* expression from chondrocytes could inhibit osteoblast differentiation by targeting *KLF5*.

Strengths and limitations

- The inhibition of *circStrn3* might be a protective response of chondrocytes to abnormal mechanical stimulation in OA. These results demonstrate that reduction of *circStrn3* causes an increase in *miR-9-5p*, which acts as a protective factor in mechanical instability-induced OA and provides a novel mechanism of communication among joint components and a potential application for the treatment of OA.
- Although we speculated that female animals would deliver similar results in our study, we did not research the related contents.

Introduction

Osteoarthritis (OA) is the most common degenerative joint disease and leading cause of physical disability in the elderly population.¹ Injuries directly leading to joint instability are highly associated with OA, suggesting that mechanical instability is a critical factor for the development of OA.²

Dysfunction of articular chondrocytes and breakdown of cartilage extracellular matrix (ECM) caused by abnormal mechanical stimulations have gained widespread acceptance as the leading causes of articular cartilage degradation.³ Recently, the pathological changes of the entire joint, including the degenerated cartilage and subchondral bone sclerosis, have become the impetus for generally recognizing OA as a disease of the joint as an organ. Mounting evidence has suggested that cartilage degeneration and subchondral bone sclerosis not only were independent drivers of pain, poor function, and structural progression of OA, but also influenced each other through proinflammatory mediators, growth factors, cytokines, and direct cell interactions.⁴

Circular RNAs (circRNAs), a novel class of endogenous noncoding RNAs,⁵ can regulate gene expression at the transcriptional or post-transcriptional level through competitively ‘sponging’ microRNAs (miRNAs). miRNAs play an important regulatory role in cell differentiation, apoptosis, and cancer.⁶ miRNAs regulate gene expression through the inhibitory engagement of complementary ‘seed sequences’ within the 3′-untranslated region (3′-UTR) of target messenger RNAs (mRNAs), leading to translational inhibition and/or mRNA degradation.⁷ The circRNA-miRNA-mRNA group participates in articular cartilage degradation caused by inflammatory factors or oxidative stress. miRNA-enriched exosomes mediate cell-to-cell communications and modulate biological process.^{8,9}

In this study, minus RNA sequencing (RNA-seq) data showed that tensile strain decreased the expression of *circStrn3* in chondrocytes. *CircStrn3* expression was also downregulated in human and mouse OA cartilage tissues and chondrocytes. Moreover, this study showed

that *circStrn3* could target Kruppel-like factor 5 (*KLF5*) and competitively ‘sponge’ miRNA-9-5p, resulting in inhibiting matrix metabolism of chondrocytes. This indicates that the reduction of *circStrn3* might be a protective factor in mechanical instability-induced OA. In addition, chondrocytes could secrete exosomal *miR-9-5p* in response to the tensile strain, which could suppress the differentiation of osteoblasts by targeting *KLF5*. Finally, intra-articular (IA) injection of exosomal *miR-9-5p* clearly alleviated the progression of OA caused by destabilized medial meniscus (DMM) surgery in mice. Taken together, these results indicate a novel mechanism of communication among joint components and provide a potential application for the treatment of OA.

Methods

Human knee cartilage procurement. Normal human knee cartilage (subjects aged 55 to 88 years, six subjects total, 50% female) samples were obtained from donors with lower limb amputation. Human OA cartilage was obtained from the knees of patients with a diagnosis of advanced OA (patients aged 55 to 85 years, six subjects total, 50% female) who underwent total knee arthroplasty. Non-OA cartilage is defined as cartilage with no histological evidence of degeneration. OA specimens obtained at the time of surgery were examined by the authors and confirmed to have gross evidence of OA (thinning or localized loss of cartilage and focal eburnation) and the histological diagnosis of OA. All patients gave informed consent.

Animal experiments. Adult male C57BL/6 mice were used to induce OA model by DMM surgery (four groups and in each group n = 6, eight weeks old), following the transection of the medial meniscotibial ligament as previously described.¹⁰ The animals were kept in a wire-topped plastic cage in an accredited animal facility in a controlled environment (mean temperature 21°C (standard deviation (SD) 1°C), mean humidity 55% (SD 10%), ventilation air volume exchanged 20 times per hour, alternating 12-hour light and dark cycles). They were allowed free access to water and standard laboratory rodent nutrition. In sham operation group, mice were operated on by opening the joint capsule only. At one week after DMM surgery, 5 µl of exosomes isolated from *miR-9-5p* overexpressed chondrocytes were intra-articularly injected once a week for the next ten weeks. Injection of exosomes isolated from negative control (miR-NC) overexpressed chondrocytes was used as control. Mice were killed 12 weeks after DMM surgery. We have included an ARRIVE checklist to show that we have conformed to the ARRIVE guidelines.

RNA fluorescence in situ hybridization and immunofluorescence. The *circStrn3* and *miR-9-5p* staining kits for tissues and cells were purchased from GenePharma (China), and the procedure of the staining was performed according to the instructions. Immunofluorescence staining was obtained by previous protocol.¹¹ The cells were incubated with mouse anti-collagen type II (COL2) antibody (1:100, Abcam Cat# ab34712, RRID: AB_731688), anti-matrix

Table I. Primers for quantitative real-time polymerase chain reaction analysis.

Gene	Forward primer	Reverse primer
<i>Col2</i>	5'-TACTGGAGTGACTGGTCTAAG-3'	5'-AACACCTTTGGACCATCTTTT-3'
<i>MMP-13</i>	5'-CTTCTGATGATGACGTTCAAG-3'	5'-GTCACACTTCTCTGGTGTTTTG-3'
<i>ADAMTSS</i>	5'-GGCAAATGTGTGGACAAAATA-3'	5'-GAGGTGCAGGGTATTACAATG-3'
<i>ALP</i>	5'-AGATGACTACAGCCAAGT-3'	5'-CTCCACGAAGAGGAAGAAG-3'
<i>RUNX2</i>	5'-TACTATGGCACTTCGTGAGGA-3'	5'-GATTTCATCCATTCTGCCACTA-3'
<i>Osterix</i>	5'-CAGGCTATGCTAATGATTACC-3'	5'-GGCAGACAGTCAGAAGAG-3'
<i>circPdia5</i>	5'-GCGGCTCCGTTTATCACCTG-3'	5'-GTCTGAAGTCATGGGGCGTG-3'
<i>circInpp5f</i>	5'-CTGCTGCTGTGCTAACGC-3'	5'-CCTGCTGATGGAGTCACCGT-3'
<i>circAdcy5</i>	5'-ATGCCTGTGTGAAGCATCCTG-3'	5'-AACTTGTCAAAGCGGGCGAA-3'
<i>circZfp426</i>	5'-GGCCACAGTAGGGTATCAGC-3'	5'-GTCCTCTGAAGGACCTGGGAA-3'
<i>circVps41</i>	5'-GTCGTCGTAGCCAAGGAACG-3'	5'-CAAACAGCAGCAGCAGACTCTT-3'
<i>circDdx26b</i>	5'-TGGCGACAGGCTTTTGACAG-3'	5'-GGCGTGATTTTCCCTCCAAC-3'
<i>circPak1</i>	5'-AAAACCCACAGGCTGTCTGG-3'	5'-AGCAGCAGCAGCTACAAGTG-3'
<i>circClec16a</i>	5'-CCGCCACGAAGTCAAGAAATG-3'	5'-TGGTACAGGTACCTTTGTTATGAGA-3'
<i>circDnmt3a</i>	5'-AGACTGGCCTTCTCGACTCC-3'	5'-GATACAAATGCTGTAGCAATCCCA-3'
<i>circPhka2</i>	5'-GTTGAGCACTGCCAGAACC-3'	5'-GCATTCTTGGCGTAGGCCAT-3'
<i>circTjp1</i>	5'-ATTCAGGTCGCTCGCATGAC-3'	5'-ATTGCTGTGCTCTGCCATTG-3'
<i>circPhc3</i>	5'-TCAGCCAACGAGACCTTCT-3'	5'-TGTGGTCTTAAACCTGGTGC-3'
<i>circEgf</i>	5'-TCTGTGTTGGAGGGAGCGA-3'	5'-TGCAAAATATATCTGCCCTTGG-3'
<i>circSenp1</i>	5'-TAAGCCTGCCCAAGTCCAT-3'	5'-ACAGAATCCTTCTGTGTGTC-3'
<i>circCabin1</i>	5'-CAGCAAGACTCACCGGAACC-3'	5'-GTCTGGCTTCGGTGTGAA-3'
<i>circStrn3</i>	5'-CCGCAACAGTACACGATCCC-3'	5'-GTAAAAATGCAATCCGTGCCTG-3'
<i>circIft88</i>	5'-AGCGTCTTTGTGTGGGTTA-3'	5'-TGCTCTCACTGCTGTATCG-3'
<i>circNnt</i>	5'-CTCAACAGTCAAGGAGGTGG-3'	5'-CATTGAAGCCCTGCTTGACCA-3'
<i>circRims1</i>	5'-CATCACAGCTCAGCCAGACAG-3'	5'-CTATACTGCCGCTCCGACC-3'
<i>circCasd1</i>	5'-GGGAGCAAGCAGCAATGA-3'	5'-TCATACAACGTGAGGTTGCCA-3'
<i>GAPDH</i>	5'-AGGTCCGGTGAACCGATTG-3'	5'-TGTAGACCATGTAGTTGAGGTCA-3'
<i>KLF5-3'-UTR</i>	5'-CGCTCAGCGAGCGAGCGCTGCCA-3'	5'-ATAAGAATGCGCCGCTGCCAATCGGTTGTTTACC-3'

ADAMTSS, a disintegrin and metalloproteinase with thrombospondin motifs 5; ALP, alkaline phosphatase; Col2, collagen type II; GAPDH, glyceraldehyde 3-phosphate dehydrogenase; KLF5, Kruppel-like factor 5; MMP, matrix metalloproteinase; RUNX2, runt-related transcription factor 2; 3'-UTR, 3'-untranslated region.

Table II. MicroRNA primers for quantitative real-time polymerase chain reaction analysis.

MicroRNA	RT-Primer	Primer
<i>miR-9-5p</i>	5'-GTCGTATCCAGTGCCTGTCTGGA GTCGGCAATTGCACTGGATACGACTCATACA-3'	F: 5'-GGGTCTTTGGTTATCTAGCTG-3' R: 5'-CAGTCCGTGCTGGAGT-3'
<i>mmu-U6</i>	5'-CGCTTCACGAATTTGCGTGCAT-3'	F: 5'-CAAAGTGCTTACAGTGCAGGTAG-3' R: 5'-CTACCTGCACTGTAAGCACTTTG-3'

miR, microRNA; mmu-U6, Mus musculus U6; RT-Primer, reverse transcription primer.

metalloproteinase (MMP)-13 antibody (1:100, Abcam Cat# ab39012, RRID: AB_776416), and anti-runt-related transcription factor 2 (RUNX2) antibody (1:200, Abcam Cat# ab76956, RRID: AB_1565955; all Abcam, UK), followed by fluorescence-linked secondary antibodies for one hour.

qRT-PCR detecting system and RNA sequencing. Total RNA from tissues and cells was extracted using Trizol reagent (Takara, Japan) and synthesized into complementary DNA (cDNA) by a Revert-Aid First Strand cDNA Synthesis Kit (Takara). Quantitative real-time polymerase chain reaction (qRT-PCR) was applied using the SYBR Premix Ex Tag Kit (Takara). The primer sequences are described in Tables I and II.

Three samples from mechanically loaded chondrocytes and three samples from non-mechanically loaded chondrocytes were collected for RNA-seq. RNAs were harvested using the miRNeasy kit (Qiagen, Germany) and RNA quality was assessed using an Agilent Bioanalyzer (Agilent, USA). High-quality (Agilent Bioanalyzer RNA integrity number > 7.0) total RNAs were employed for the preparation of sequencing libraries using Illumina TruSeq Stranded Total RNA/Ribo-Zero Sample Prep Kit purchased from GenePharma (China). A total of 500 to 1,000 ng of riboRNA-depleted total RNA was fragmented by RNase III treatment at 37°C for 15 minutes, and RNase III was inactivated at 65°C for ten minutes. Size selection (50 to 150 bp fragments) was performed using the FlashPAGE

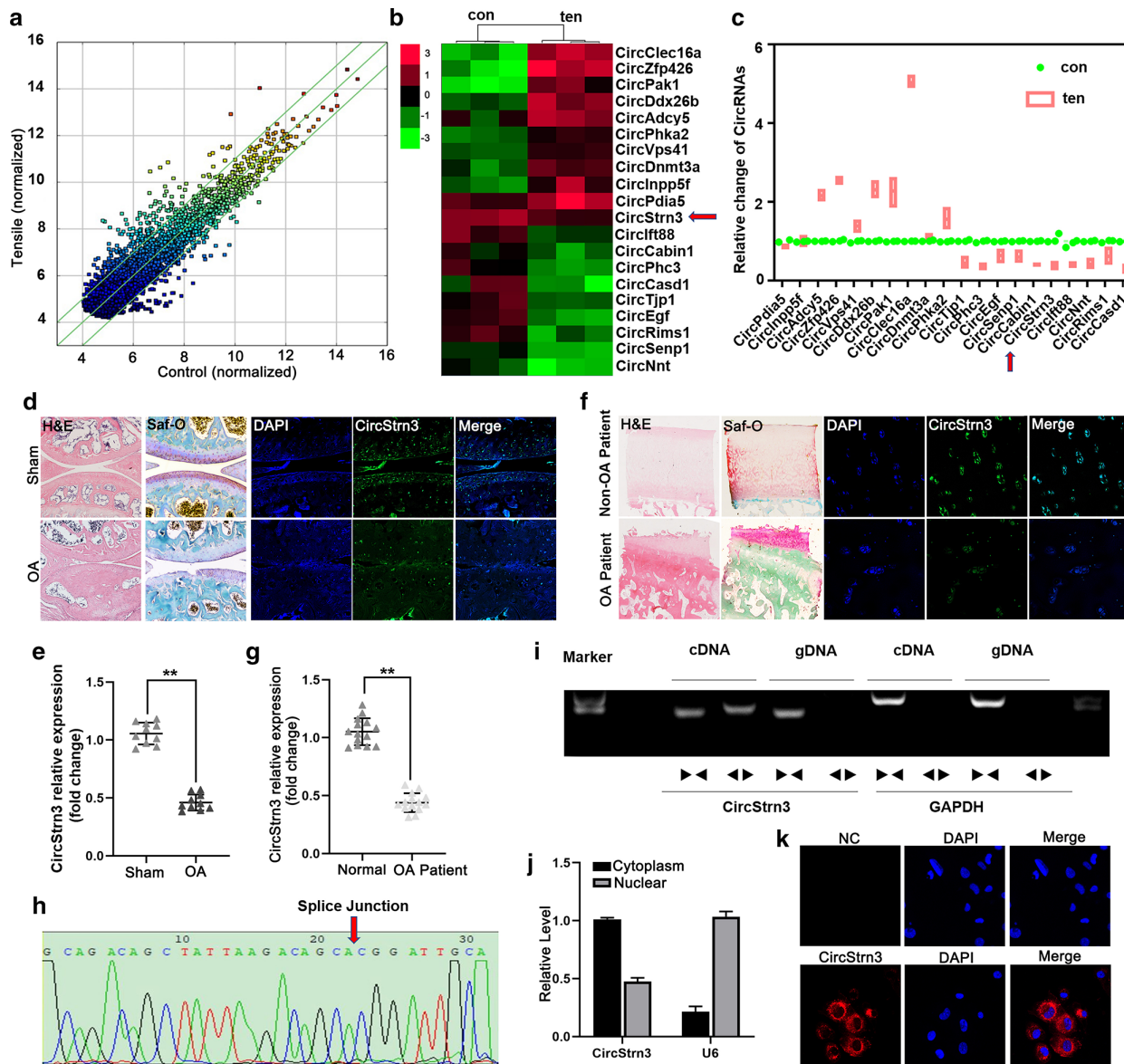


Fig. 1

CircStrn3 was decreased in knee articular cartilage from osteoarthritis (OA) patients and mice. a) Differentially expressed circular RNAs (circRNAs) found by ribo-minus RNA sequencing (RNA-seq). $n = 3$. b) Heat map representation of circRNAs differentially expressed in mechanically loaded chondrocytes. Red indicates circRNAs induced, and green indicates circRNAs repressed. ($n = 3$). c) RNA-seq results were validated by quantitative real-time polymerase chain reaction (qRT-PCR) in mechanically loaded chondrocytes. d) Haematoxylin and eosin (H&E) staining and Safranin-O (Saf-O)/Fast Green staining were applied to observe morphological structure of the articular cartilage in OA mice. Fluorescence in situ hybridization (FISH) staining results showed that *circStrn3* was downregulated in OA mice cartilage. ($n = 4$, scale bar: $10 \mu\text{m}$). e) The results of qRT-PCR show that expression of *circStrn3* was decreased in chondrocytes from OA mice. ($n = 4$, $**p < 0.01$). f) H&E staining and Safranin-O/Fast Green staining were applied to observe morphological structure of the articular cartilage in OA patients. FISH staining results showed that *circStrn3* was downregulated in OA patients. ($n = 6$, scale bar: $10 \mu\text{m}$). g) The results of qRT-PCR showed that expression of *circStrn3* was decreased in chondrocytes from OA patients. ($n = 6$, $**p < 0.01$). h) Divergent primers detected circular RNAs in complementary DNA (cDNA), but not in genomic DNA (gDNA). i) Sanger sequencing showed the back-splice junction (arrow) of *circStrn3*. j) *CircStrn3* expression was measured in nuclear and cytoplasmic separation by qRT-PCR in chondrocytes. ($n = 4$, $**p < 0.01$). k) FISH staining results show that *circStrn3* was downregulated in mechanically loaded chondrocytes ($n = 4$, scale bar: $10 \mu\text{m}$). Independent-samples *t*-test was used to compare data between two groups, and one-way analysis of variance was used for comparison between multiple groups. con, control group; DAPI, 4',6-diamidino-2-phenylindole; GAPDH, glyceraldehyde 3-phosphate dehydrogenase; NC, negative control; ten, mechanically loaded chondrocytes group.

denaturing PAGE-fractionator (Life Technologies, Thermo Fisher Scientific, USA) prior to ethanol precipitation overnight. The total RNA samples were sent for sequencing at BioMarker (China) and the data analyzed at BioMarker platform.¹²

Western blotting analysis. Radioimmunoprecipitation assay (RIPA) buffer mixed with protease and phosphatase inhibitor mixtures was used to extract the proteins, and the proteins were then transferred onto polyvinylidene fluoride (PVDF) membranes (MilliporeSigma, USA) after

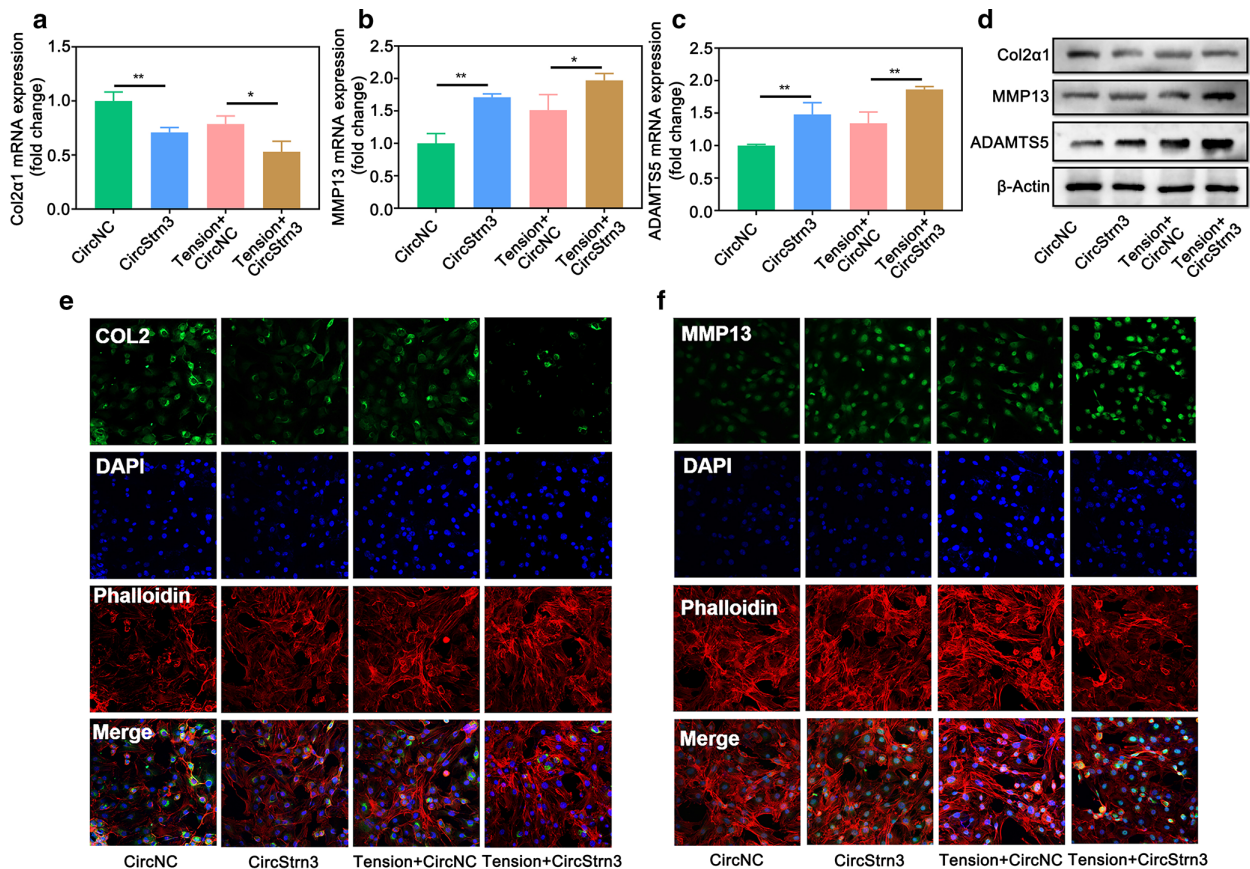


Fig. 2

CircStrn3 was involved in the regulation of chondrocyte extracellular matrix production by mechanical stress. a) to c) Quantitative real-time polymerase chain reaction (qRT-PCR) tested the messenger RNA (mRNA) expressions of COL2a1, matrix metalloproteinase-13 (MMP-13), and a disintegrin and metalloproteinase with thrombospondin motifs 5 (ADAMTS5) in chondrocytes transfected with *circStrn3* or circNC, followed by stimulation of tensile strain or control condition (n = 4, *p < 0.05, **p < 0.01). d) Western blot tested the expressions of COL2a1, MMP-13, and ADAMTS5 in chondrocytes transfected with *circStrn3* or circNC, followed by stimulation of tensile strain or control condition (n = 4). e) and f) Immunofluorescence assay tested the expressions of COL2a1 and MMP-13 in chondrocytes transfected with *circStrn3* or circNC, followed by stimulation of tensile strain or control condition (n = 4, scale bar: 10 μm). Independent-samples *t*-test was used to compare data between two groups, and one-way analysis of variance was used for comparison between multiple groups. DAPI, 4',6-diamidino-2-phenylindole; mRNA, messenger RNA; NC, negative control.

separation by sodium dodecyl sulphate-polyacrylamide gel electrophoresis (SDS-PAGE) (7.5% to 12.5% polyacrylamide gels). Primary antibodies were anti-COL2a1 antibody (1:1,000, Abcam Cat# ab34712, RRID: AB_731688), anti-MMP-13 antibody (1:1,000, Abcam Cat# ab39012, RRID: AB_776416), anti-a disintegrin and metalloproteinase with thrombospondin motifs 5 (ADAMTS5) antibody (1:250, Abcam Cat# ab41037, RRID: AB_2222327), anti-β-actin antibody (1:1,000, Abcam Cat# ab8226, RRID: AB_306371), and anti-*KLF5* antibody (1:2,000, Abcam Cat# ab137676, RRID: AB_2744553; all Abcam). Secondary antibody was rabbit anti-mouse IgG H&L antibody (1:5,000, Abcam Cat# ab6728, RRID: AB_955440; Abcam). Primary and secondary antibodies were used to detect the corresponding proteins. The results were obtained using the Enhanced Chemiluminescence (ECL) Western blot System (Amersham Biosciences, China).

Isolation and identification of chondrocyte-derived exosomes. The exosomes were separated from 200 ml of chondrocyte culture medium. The isolation and

purification process was conducted as previously described.¹³ Briefly, the culture supernatant was obtained by centrifugation at 300× g and 2,000× g separately for ten minutes to remove the floating and dead cells. The supernatant was then centrifugated at 10,000× g for 30 minutes to remove cell debris. This was followed by centrifugation at 10,000× g for 70 minutes, and the pellets were exosomes and contaminating proteins. The pellets were washed with phosphate-buffered saline (PBS) and subjected to centrifugation at 10,000× g for 70 minutes again, and the last pellets were the pure exosomes.

In order to identify the exosome, we extracted and observed the morphology of exosome by conducting the transmission electron microscopy (TEM) test. Exosomes were fixed with 1% (w/v) glutaraldehyde in PBS. A drop of the mixture was loaded onto a carbon-coated grid, negatively stained with 3% (w/v) aqueous phosphotungstic acid for one minute, and then observed under TEM (HT7700; Hitachi, Japan). The collected exosomes were resuspended with 1 ml PBS and loaded into the

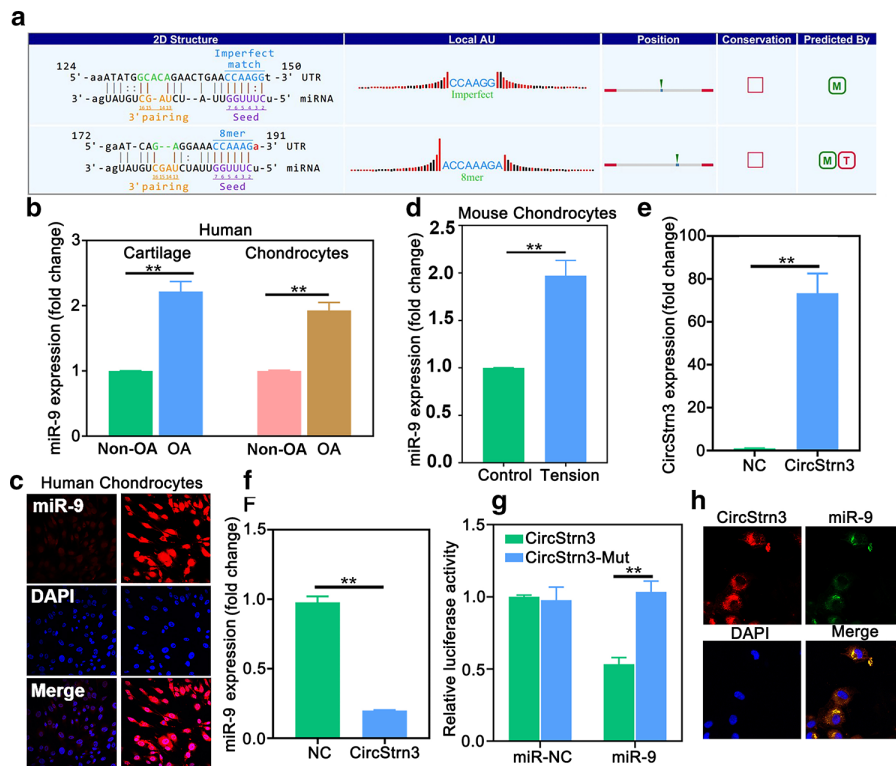


Fig. 3

CircStrn3 was involved in the regulation of chondrocyte extracellular matrix production by mechanical stress. a) Complementation between *circStrn3* and 'seed sequence' of microRNA (miR)-9-5p. b) The results of quantitative real-time polymerase chain reaction (qRT-PCR) showed that expression of *miR-9-5p* was increased in cartilage and chondrocytes from osteoarthritis (OA) patients ($n = 4$, $**p < 0.01$). c) Fluorescence in situ hybridization (FISH) staining results showed that *miR-9-5p* was upregulated in human chondrocytes ($n = 4$, scale bar: 10 μm). d) qRT-PCR tested the expression of *miR-9-5p* in chondrocytes exposed to mechanical loading or control condition ($n = 4$, $**p < 0.001$). e) to f) qRT-PCR tested the expressions of e) *circStrn3* and f) *miR-9-5p* in chondrocytes transfected with *circStrn3* or *circNC* ($n = 4$, $**p < 0.01$). g) The results showed a significant decrease in firefly luciferase activity when wild type (WT) was cotransfected with *miR-9-5p* mimics, thus no significant change was observed in luciferase activity after co-transfection with mutation type (Mut) and *miR-9-5p* mimic ($n = 4$, $**p < 0.01$). h) FISH staining results showed that *circStrn3* colocalized with *miR-9-5p* in the cytoplasm. ($n = 6$, scale bar: 10 μm). Independent-samples *t*-test was used to compare data between two groups, and one-way analysis of variance was used for comparison between multiple groups. DAPI, 4',6-diamidino-2-phenylindole; NC, negative control.

sample pool of Nanosight LM 10 (Malvern Panalytical) as instructed. After the sample measurement was completed, the particle size distribution was calculated. The fluorescent dye 3,3'-diocadecyloxycarbocyanine perchlorate (DiO) (Life Technologies, USA) was used to label exosomes and cell membrane.

Chondrocyte culture and tensile strain loading. Chondrocytes were isolated from articular cartilage in the knee joints of mice and human as previously reported.¹⁴ Articular cartilage tissues were cut into small pieces ($< 1 \text{ mm}^3$) and digested with 0.25% trypsin for 30 minutes, followed by digestion with 0.2% type II collagenase for four hours. The released cells were cultured in Dulbecco's Modified Eagle Medium (DMEM)/F12 media supplemented with 10% fetal bovine serum (FBS) and antibiotics. After reaching 80% confluence, the cells were subjected to cyclic tensile strain with a 0.5 Hz sinusoidal curve at 5% to 20% elongation for 12 to 48 hours using Flexcell1 FX-5000 Tension System as described in the manufacturer's manual (Flexcell International Corporation, USA). Only cells with fewer than two passages were used in order to preserve chondrocyte phenotype.

Cell transfection. The overexpression plasmid vector for mouse *circStrn3* and mouse *KLF5* gene was created by GeneChem (China). *miR-9-5p* mimic, miR-NC, and anti-miRNA oligonucleotides (AMO)-9-5p and AMO-NC were synthesized by GeneChem. Chondrocytes were transfected with *miR-9-5p*, AMO-9-5p, or plasmid DNA using Lipofectamine 3000 reagent (Invitrogen, Thermo Fisher Scientific, UK) according to the manufacturer's protocols. **Luciferase reporter assays.** *CircStrn3* sequence containing the putative (wild type (WT)) or mutation (mutation type (Mut)) target sites for *miR-9-5p* was synthesized and cloned into the psiCHECK2 reporter vector (Promega Corporation, USA) downstream to the firefly luciferase. After 24 hours of starvation in serum-free medium, HEK293 cells (1×10^5 per well) were transfected with WT or Mut and cotransfected with 100 nM *miR-9-5p* mimics or miR-NC using Lipofectamine 3000 reagent. The cells were also transfected with 50 ng pRL-TK vector as an internal standard.

The 3'-UTR sequences of *KLF5* predicted to interact with *miR-9-5p* were identified using TargetScan.¹⁵ DNA fragment of the 3'-UTR of *KLF5* containing the

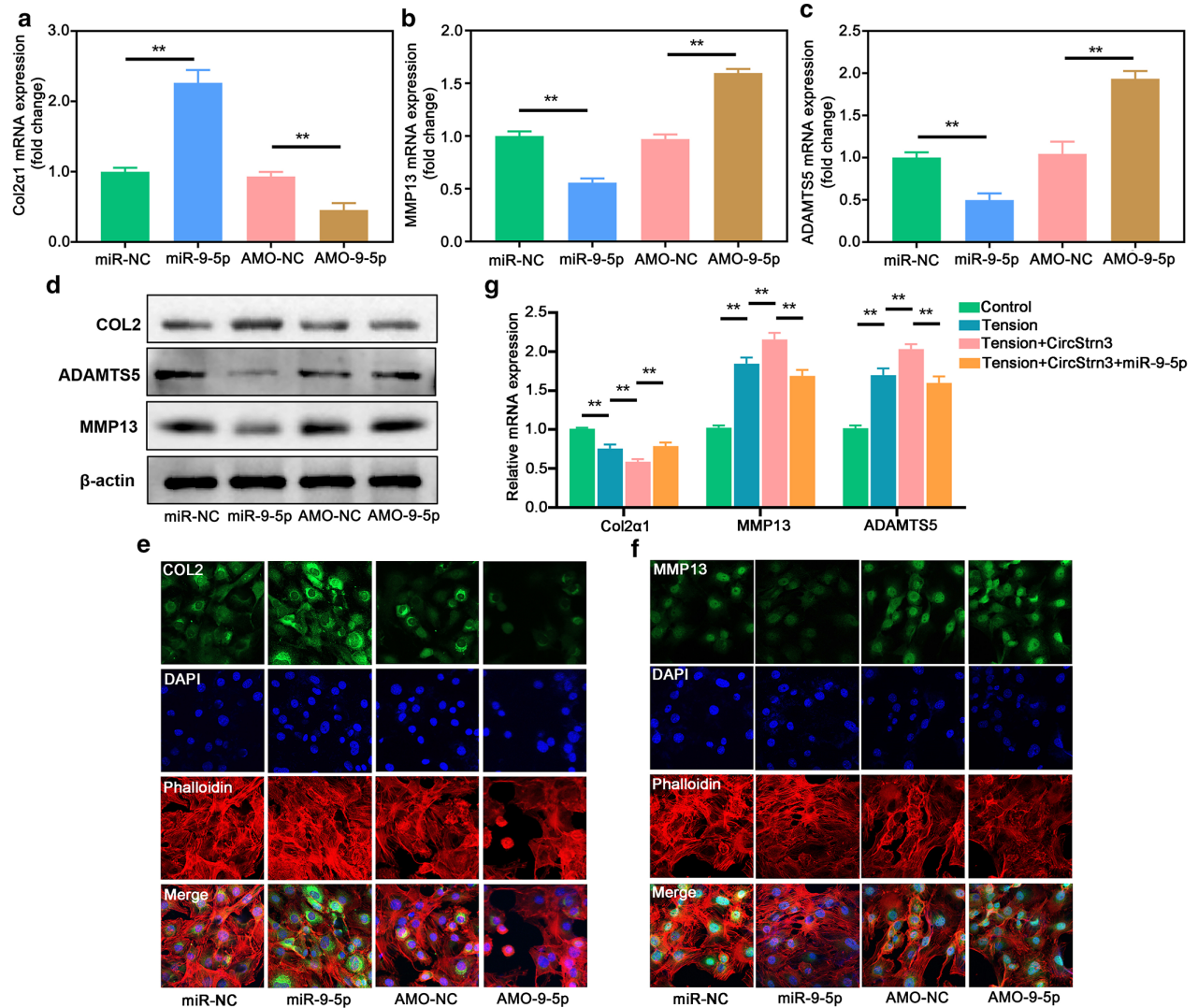


Fig. 4

MicroRNA (miR)-9-5p was involved in the regulation of chondrocyte extracellular matrix production. a) to c) Quantitative real-time polymerase chain reaction (qRT-PCR) tested the messenger RNA (mRNA) expressions of COL2α1, matrix metalloproteinase (MMP)-13, and a disintegrin and metalloproteinase with thrombospondin motifs 5 (ADAMTS5) in chondrocytes transfected with *miR-9-5p* mimic and anti-miRNA oligonucleotide (AMO)-9-5p ($n = 4$, $**p < 0.01$). d) Western blot tested the expressions of COL2α1, MMP-13, and ADAMTS5 in chondrocytes transfected with *miR-9-5p* mimic and AMO-9-5p ($n = 4$). e) and f) Immunofluorescence assay tested the expressions of COL2α1 and MMP-13 in chondrocytes transfected with *miR-9-5p* mimic and AMO-9-5p ($n = 4$; scale bar: 10 μm). g) qRT-PCR tested the mRNA expressions of COL2α1, MMP-13, and ADAMTS5 in chondrocytes transfected with *miR-9-5p* mimics or *circStrn3*, followed by stimulation of tensile strain or control condition ($n = 4$, $**p < 0.01$). Independent-samples *t*-test was used to compare data between two groups, and one-way analysis of variance was used for comparison between multiple groups. DAPI, 4',6-diamidino-2-phenylindole; NC, negative control.

putative *miR-9-5p* binding sequence was amplified by PCR. Forward and reverse primers for amplicon were designed to include, respectively, Xho1 and Not1 restriction enzyme recognition sites. Sequences of primers used for PCR-amplification of *KLF5* are shown in Table I. The fragment was cloned into the psiCHECK2 reporter vector (Promega Corporation) downstream to the firefly luciferase. Luciferase reporter genes were cotransfected with *miR-9-5p* mimics and *miR-NC* into HEK293 cells using Lipofectamine 3000. The cells were also transfected with 50 ng of pRL-TK vector as an internal standard. Dual-Luciferase Reporter Assay System (Promega Corporation) and a luminometer (Lumat LB9507; Berthold

Technologies, Germany) were performed to measure the relative luciferase activity.

Statistical analysis. All data were analyzed using GraphPad Prism (GraphPad Software, USA), and are presented here as mean (SD). Independent-samples *t*-test was used to compare data between two groups, and one-way analysis of variance (ANOVA) was used for comparison between multiple groups. Statistical significance was set at $p < 0.05$.

Results

CircStrn3 was decreased in knee articular cartilage from OA patients and mice. Ribo-minus RNA-seq was first applied

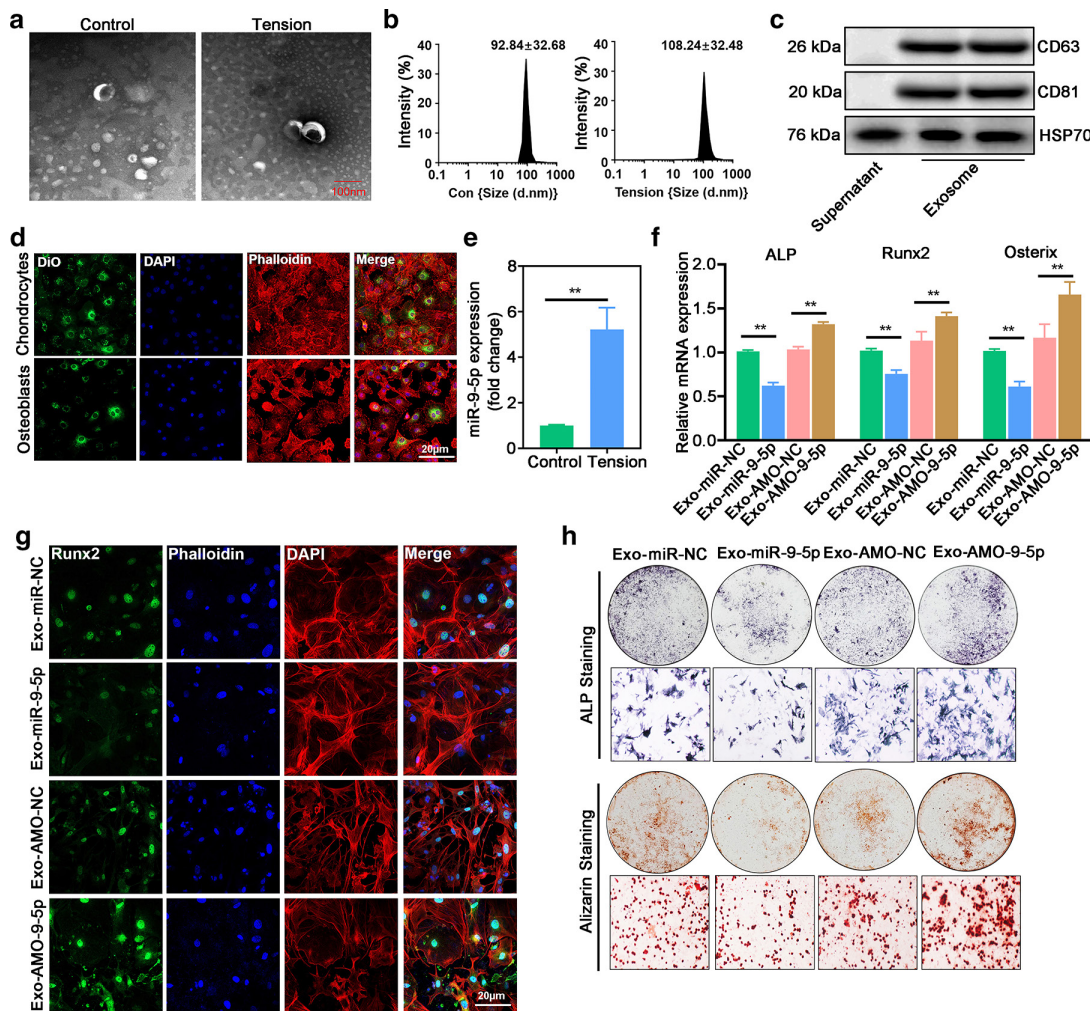


Fig. 5

Exosomal microRNA (miR)-9-5p from mechanically loaded chondrocytes inhibited osteoblast differentiation. a) Scanning electron microscope (SEM) imaging showed that the exosomes exhibited classical typical sphere-shaped bilayer membrane structure ($n = 6$, scale bar: 100 nm). b) SEM imaging showed that the mean size distribution of isolated exosomes was 92.84 nm (standard deviation 32.68) in chondrocytes ($n = 6$). c) Western blot tested the expressions of CD63, CD81, and HSP70 in exosomes ($n = 4$). d) Confocal imaging showed numerous 3',3'-dioctadecyloxycarbocyanine perchlorate (DiO) particles observed within osteoblasts. Green: chondrocytes labelled by Vybrant DiO. Blue: 4',6-diamidino-2-phenylindole (DAPI) labelling of cell nuclei. Red: cytoskeleton labelled by phalloidin ($n = 4$; scale bar: 20 μm). e) The results of quantitative real-time polymerase chain reaction (qRT-PCR) showed that expression of *miR-9-5p* was increased in chondrocytes stimulated with tensile strain ($n = 4$, $**p < 0.01$). f) qRT-PCR tested the messenger RNA (mRNA) expressions of alkaline phosphatase (ALP), runt-related transcription factor 2 (RUNX2), and *Osterix* in osteoblasts adding exosomes from chondrocytes transfected with *miR-9-5p* or anti-miRNA oligonucleotide (AMO)-9-5p ($n = 4$, $**p < 0.01$). g) Immunofluorescence assay tested the expressions of RUNX2 in osteoblasts adding exosomes from chondrocytes transfected with *miR-9-5p* or AMO-9-5p ($n = 4$; scale bar: 20 μm). h) Osteoblasts adding exosomes from chondrocytes transfected with *miR-9-5p* or AMO-9-5p. ALP and Alizarin red S (ARS) staining were performed after seven and 14 days of induction, respectively ($n = 4$; scale bar: 10 μm). Independent-samples *t*-test was used to compare data between two groups, and one-way analysis of variance was used for comparison between multiple groups. NC, negative control.

to screen dysregulated circRNAs in mechanically loaded chondrocytes. The 20 most differentially expressed ($p < 0.05$, fold change > 3) circRNAs were then identified (Figures 1a and 1b). qRT-PCR showed that in these differentially expressed circRNAs, *circStrn3* was the most frequently repressed (Figure 1c). Thus, *circStrn3* was first selected for further study. Haematoxylin and eosin (H&E) staining and Safranin-O/Fast Green staining showed that articular cartilage in sham group mouse and non-OA patients possessed regular morphological structure. In contrast, OA group mice and OA patients clearly exhibited reduced chondrocyte and articular cartilage thickness, and

articular cartilage possessed an irregular morphological structure (Figures 1d to 1f). The expression of *circStrn3* was tested using fluorescence in situ hybridization (FISH) in knee articular cartilage from OA patients (Figure 1f) and OA group mice (Figure 1d). The results show that *circStrn3* expression was significantly decreased. We isolated and cultured the chondrocytes from Sham group mice and OA group mice, followed by the analysis of qRT-PCR to test *circStrn3* expression. The results show that the expression of *circStrn3* was decreased in chondrocytes from the OA group mice (Figure 1e). Similar results were also obtained from OA patients (Figure 1g). Next, we

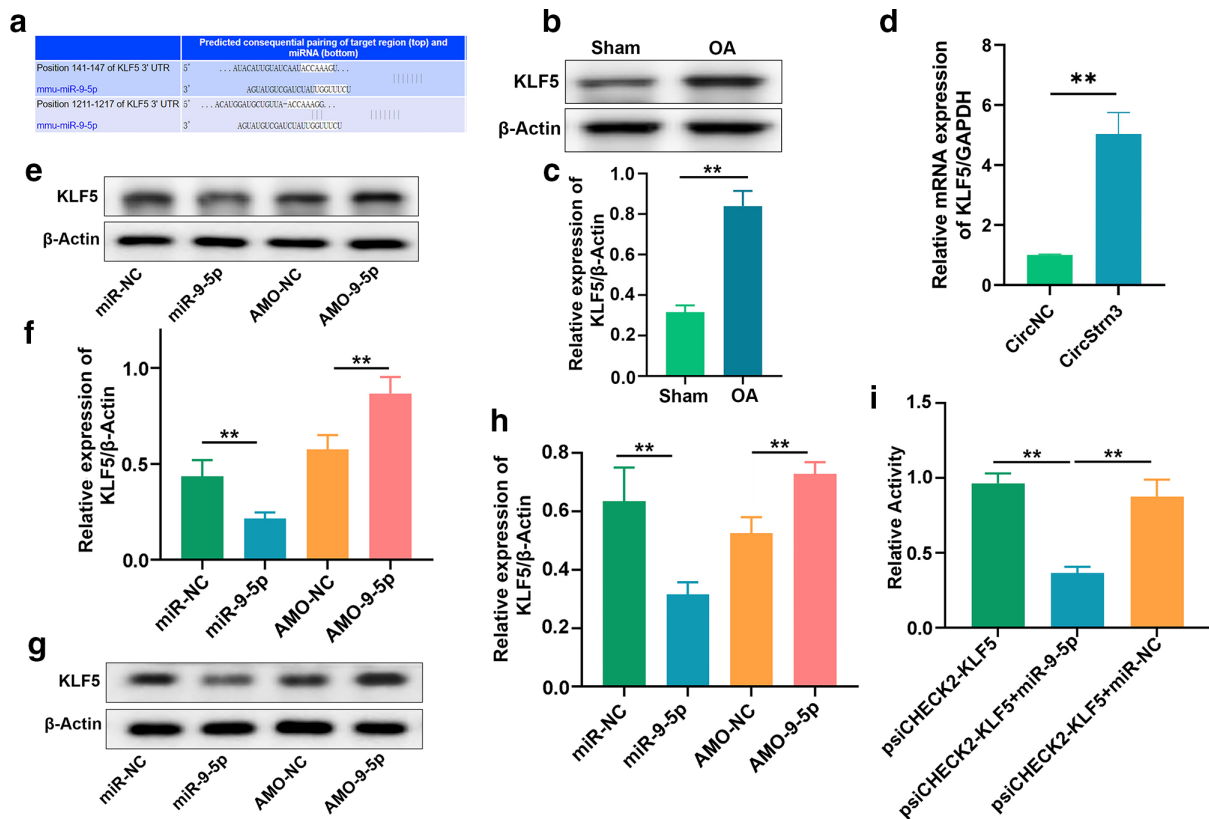


Fig. 6

The identification of molecular target of microRNA (miR)-9-5p. a) MicroRNA complementarity of *miR-9-5p* targeting Kruppel-like factor 5 (*KLF5*). b) to c) The results of western blot show that expression of *KLF5* was increased in chondrocytes from osteoarthritis (OA) mice compared to sham mice ($n = 4$, $**p < 0.01$). d) The results of quantitative real-time polymerase chain reaction (qRT-PCR) show that expression of *KLF5* was increased by the overexpression of *CircStrn3* in chondrocytes ($n = 4$, $**p < 0.01$). e) to h) The results of western blot show the level of *KLF5* expression in e) to f) chondrocytes and g) to h) osteoblasts transfected with *miR-9-5p* or anti-miRNA oligonucleotide (AMO)-9-5p ($n = 4$, $**p < 0.01$). i) Luciferase activity was diminished in the reporter containing the 3'-untranslated region (3'-UTR) of *KLF5* treated with *miR-9-5p* compared with *pMIR-KLF5* alone ($n = 4$, $**p < 0.01$). Independent-samples *t*-test was used to compare data between two groups, and one-way analysis of variance was used for comparison between multiple groups. GAPDH, glyceraldehyde 3-phosphate dehydrogenase; mRNA, messenger RNA; NC, negative control.

designed a set of convergent primers by *strn3* mRNA and divergent primers for *circStrn3* amplification using cDNA and genomic DNA (gDNA). *CircStrn3* was amplified by divergent primers in cDNA but not in gDNA (Figure 1i). We used Sanger sequencing of the RT-PCR product amplified by divergent primers to confirm the head-to-tail splicing junction of *circStrn3* (Figure 1h), which indicated that *circStrn3* could be expressed in chondrocytes. We thus determined that *circStrn3* is primarily located in cytoplasm by performing FISH experiments and nuclear and cytoplasmic separation qRT-PCR in chondrocytes (Figures 1j and 1k).

***CircStrn3* was involved in the regulation of chondrocyte ECM production by mechanical stress.** COL2 α 1, as a major component of the cartilage ECM, was decreased in *circStrn3* overexpressed chondrocytes. However, MMP-13 and ADAMTS5, two critical enzymes for cartilage degrading, were significantly increased in chondrocytes overexpressed with *circStrn3*. qRT-PCR and western blot analysis showed that decreasing expression of COL2 α 1 and increasing expressions of MMP-13 and ADAMTS5 were observed in mechanically loaded chondrocytes, which were

significantly alleviated by overexpression of *circStrn3* (Figures 2a to 2d). Similar results were further confirmed by immunofluorescence staining (Figures 2e and 2f).

***miR-9-5p* was a complementary targeting miRNA of *circStrn3*.** Some miRNAs were predicted to bind to *circStrn3*, including *miR-9-5p*, miR-6967-3p, and miR-667-5p (data not shown). Complementation between *circStrn3* and 'seed sequence' of *miR-9-5p* is shown in Figure 3a. Among these miRNAs, the expression of *miR-9-5p* was increased (Figure 3b). FISH assay in chondrocytes also confirmed that *miR-9-5p* was abundant in OA patients (Figure 3c). In addition, qRT-PCR results showed an increasing expression of *miR-9* in mouse chondrocytes exposed to mechanical loading, which corresponded to the regulation of *circStrn3* (Figure 3d). We transfected the mouse chondrocytes with *circStrn3* overexpression plasmid, and qRT-PCR results showed that *miR-9-5p* was significantly decreased (Figures 3e and 3f). The sequence of *circStrn3* was inserted into the 3'-UTR of the psiCHECK2 plasmid (WT) to construct dual-luciferase reporter system. The results showed a significant decrease in the firefly luciferase activity when WT was cotransfected with *miR-9-5p*

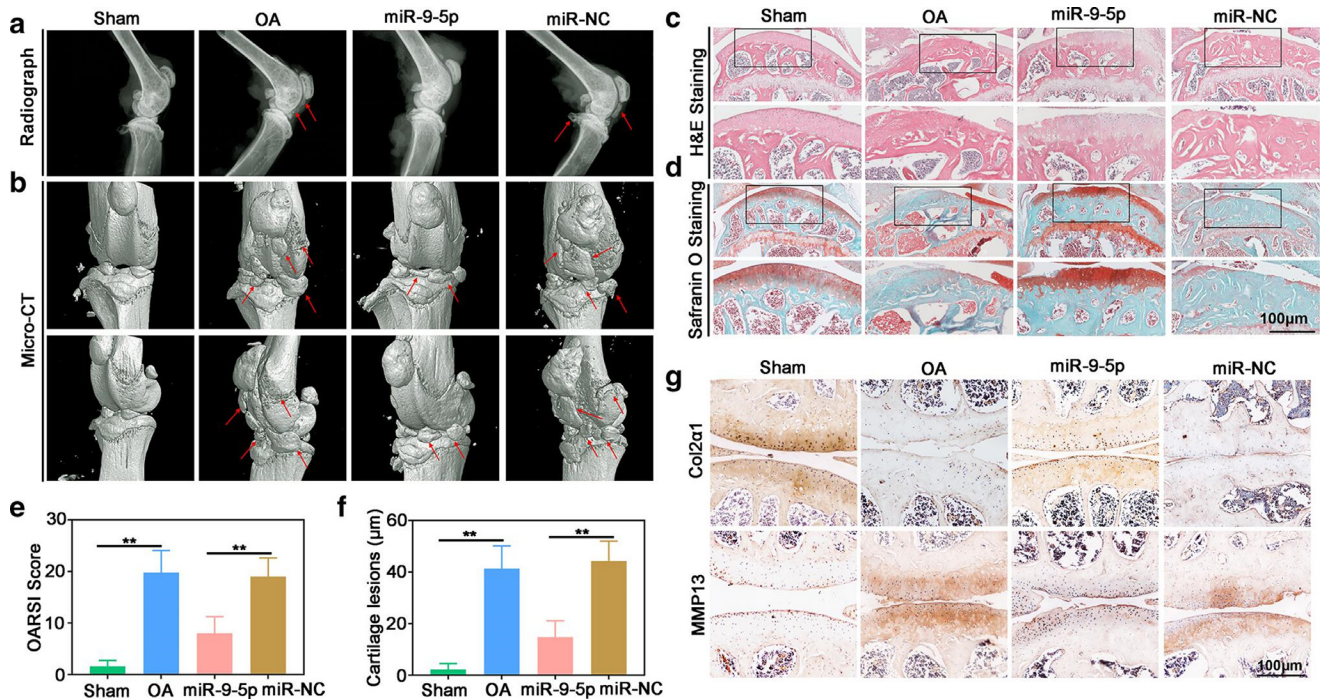


Fig. 7

Therapeutic effect of microRNA (miR)-9-5p in destabilized medial meniscus (DMM)-induced osteoarthritis (OA) mice. a) Radiographs and b) micro-CT imaging for morphological structure in knee of OA mouse at 12 weeks post-DMM surgery, followed by treatment with intra-articular (IA) injection of exosomes with high *miR-9-5p* expression and *miRNA-NC*, respectively (n = 4). c) and d) Haematoxylin and eosin (H&E) staining and Safranin-O/Fast Green staining of articular cartilage tissues of OA mouse at 12 weeks post-DMM surgery, followed by treatment with IA injection of exosomes with high *miR-9-5p* expression and *miRNA-NC*, respectively (n = 4; scale bar: 100 µm). e) and f) Results of Safranin-O/Fast Green staining of e) Osteoarthritis Research Society International (OARSI) score and f) depth of cartilage lesions (n = 4). g) Immunohistochemistry staining showed the intensity of immunostaining of COL2a1 and matrix metalloproteinase (MMP)-13 at 12 weeks post-DMM surgery, followed by treatment with IA injection of exosomes with high *miR-9-5p* expression and *miRNA-NC*, respectively (n = 4; scale bar: 100 µm). Independent-samples t-test was used to compare data between two groups, and one-way analysis of variance was used for comparison between multiple groups. NC, negative control.

mimics (Figure 3g). We cloned two mutated sequences into 3'-UTR of psiCHECK2 plasmid (Mut), which were binding sites for *miR-9-5p* in mutated *circStrn3*. No significant change was observed in luciferase activity after cotransfection with Mut and *miR-9-5p* mimic (Figure 3g). Next, we performed FISH and confirmed that *circStrn3* colocalized with *miR-9-5p* in the cytoplasm (Figure 3h).

miR-9-5p was overexpressed or silenced in chondrocytes with *miR-9-5p* mimic and AMO-9-5p, respectively. qRT-PCR analysis indicated that the expression of COL2a1 was increased, and the expressions of MMP-13 and ADAMTS-5 were obviously decreased in chondrocytes transfected with *miR-9-5p* mimics compared to NC group, Also, the results were completely opposite when chondrocytes were transfected with AMO-9-5p (Figures 4a to 4c). Similar results were obtained by western blot analysis (Figure 4d) and immunofluorescence assay (Figures 4e and 4f). We found that overexpression of *circStrn3* promoted the downregulation of COL2a1 expression and upregulation of MMP-13 and ADAMTS5 expressions, which could be attenuated by overexpression of *miR-9-5p* (Figure 4g).

Exosomes with high *miR-9-5p* from chondrocytes inhibited osteoblast differentiation. The scanning electron microscope (SEM) imaging showed that the exosomes

exhibited classical typical sphere-shaped bilayer membrane structure (Figure 5a). The mean size distribution of isolated exosomes was 92.84 nm (SD 32.68) in chondrocytes (Figure 5b). Western blot analysis of exosome markers in the extracts confirmed the presence of exosomes (Figure 5c). The chondrocytes were labelled using green fluorescent lipophilic dye (Vybrant DiO; Thermo Fisher Scientific, China). Osteoblasts were cocultured with chondrocytes for 24 hours. Confocal imaging showed numerous DiO particles observed within osteoblasts (Figure 5d). The level of *miR-9-5p* in osteoblasts cocultured with control chondrocytes was obviously lower than those cocultured with mechanical loaded chondrocytes (Figure 5e).

We collected exosomes from chondrocytes overexpressed with *miR-9-5p*, and added these exosomes into mesenchymal stem cells (MSCs) cultured in osteogenic differentiation medium for seven days. The results showed that the expressions of ALP, RUNX2, and *Osterix* were decreased (Figures 5f and 5g). We decreased *miR-9-5p* expression in chondrocytes with AMO-9-5p, followed by collection of exosomes. qRT-PCR and immunofluorescence analysis showed that the expressions of ALP, RUNX2, and *Osterix* were increased when compared with those transfected with AMO-NC (Figures 5f and 5g). ALP

staining and Alizarin red S staining further demonstrated that exosomes with high *miR-9-5p* from chondrocytes inhibited osteoblast differentiation, whereas inhibition of *miR-9-5p* attenuated this effect (Figure 5h).

The identification of molecular target of *miR-9-5p*. A computation- and bioinformatics-based approach was used to predict the putative targets of *miR-9-5p* through TargetScan. These explorations led to candidate targets of *miR-9-5p*: *KLF5*. The unique sites of miRNA:mRNA complementarity of *miR-9-5p* targeting *KLF5* are shown in Figure 6a. The results of western blot show that expression of *KLF5* was increased in chondrocytes from OA mice compared to sham mice (Figures 6b and 6c). The expression of *KLF5* was increased by the overexpression of *circStrn3* in chondrocytes (Figure 6d). *MiR-9-5p* obviously decreased the expression of *KLF5* in chondrocytes and osteoblasts. However, the level of *KLF5* expression was upregulated by *AMO-9-5p* (Figures 6e to 6h). We placed the 3'-UTRs of *KLF5* into the 3'-UTR of a luciferase reporter plasmid to construct chimeric vectors. Luciferase activity was diminished in the report containing the 3'-UTR of *KLF5* treated with *miR-9-5p* compared with *KLF5* alone (Figure 6i).

Therapeutic effect of miRNA-9 in DMM-induced OA mice. Radiograph images show that exacerbated OA pathology was found in DMM-operated mice, whereas injection of exosomal *miR-9-5p* into joint cavity clearly ameliorated DMM-induced OA pathology (Figure 7a). Furthermore, micro-CT (μ CT) imaging was used to determine changes in bone architecture and bone mineral density in mouse model. The reduction of chondrocytes and articular cartilage thickness with the irregular morphological structure was evident in OA mice at 12 weeks post-DMM surgery. However, injection of exosomal *miR-9-5p* into joint cavity could obviously attenuate DMM-induced OA mice (Figure 7b). H&E staining and Safranin-O/Fast Green staining (Figures 7c and 7d) were applied to evaluate the histopathology of articular cartilage tissues. Compared with the OA group and OA + *miR-NC* group, the OA + *miR-9-5p* group showed improvement of the morphological integrity, less severe lesions, and decreased surface denudation. According to the results of Safranin-O/Fast Green staining, the Osteoarthritis Research Society International (OARSI) score (Figure 7e) of OA + *miR-9-5p* group was lower than OA group and OA + *miR-NC* group. In addition, depth of cartilage lesions was reduced in the OA + *miR-9-5p* group (Figure 7f). Immunohistochemistry staining showed that COL2 α 1 was attenuated in OA mice injected with exosomal *miR-9-5p*. Conversely, injection of exosomal *miR-9-5p* into the IA joint cavity of OA mice obviously decreased the expression of MMP-13 (Figure 7g).

Discussion

CircRNAs are involved in the regulation of articular cartilage degradation caused by inflammatory factors or oxidative stress.¹⁶ In this study we rigorously document the pivotal role of *circStrn3* in cartilage development and

OA pathogenesis using RNA-seq, together with large-scale patient datasets and experimental mouse models of OA. Further studies have shown that *circStrn3* inhibited matrix metabolism of chondrocytes through competitively 'sponging' *miR-9-5p* targeting *KLF5*. Exosomes with high *miR-9-5p* expression from chondrocytes inhibited osteoblast differentiation. In a more therapeutically oriented approach, our results reveal that local IA administration of exosomal *miR-9-5p* in OA mice could maintain chondrocyte normal phenotype and even reverse cartilage degradation. Taken together, these results indicate that the *circStrn3/miR-9-5p/KLF5* network, crucial factors for articular cartilage degradation and subchondral bone sclerosis, may be used as a therapeutic target for OA.

Our results demonstrate for the first time that *circStrn3* is important in the development of OA. Indeed, *circStrn3* has been confirmed to be involved in many diseases. Ling et al¹⁷ found that knockdown of *circStrn3* effectively inhibited cell proliferation and promoted epithelial mesenchymal transition in glomerular mesangial cells. Gupta et al¹⁸ confirmed that *circStrn3* was regulated on doxorubicin treatment in the heart. Knockdown of *circStrn3* increased the susceptibility of cardiac muscle tissue to doxorubicin in cardiotoxicity. However, no studies have identified *circStrn3* as a critical factor for OA. In the present study, we found that the expression of *circStrn3* was obviously decreased in chondrocytes from OA patients and OA mice. Overexpression of *circStrn3* could promote the inhibition of chondrocyte ECM production by mechanical stress. Thus, the inhibition of *circStrn3* might be a protective response of chondrocytes to abnormal mechanical stimulation in OA.

In this study, bioinformatic tools were first used to predict the putative targeting miRNAs of *circStrn3*. *MiR-9-5p* was selected for further study based on its expression level. Kopańska et al¹⁹ found that expression of *miR-9-5p* was significantly upregulated in OA tissues (patients vs control group), which was consistent with our results. We found that *miR-9-5p* could increase the expression of COL2 α 1 and decrease the expressions of MMP-13 and ADAMTSS5. Furthermore, exosomes with high *miR-9-5p* expression inhibited osteogenic differentiation of MSCs. These results indicate that *miR-9-5p* is a protective factor for OA. Similar conclusions were also drawn in previous studies. Chen et al²⁰ found that overexpression of *miR-9-5p* suppressed chondrocyte apoptosis and promoted cartilage remodelling through downregulation of troponin C (Tnc) in mice with OA. Jin et al²¹ found that bone marrow mesenchymal stem cell (BMSC)-derived exosomal *miR-9-5p* could influence OA progression by inhibiting syndecan-1. All these studies suggested that *miR-9-5p* could alleviate OA, even if this is through different regulation pathways.

Our results show that inhibition of osteoblast differentiation by chondrocyte-derived exosomes with high *miR-9-5p* expression is an important mechanism for *miR-9-5p* to alleviate OA. The effects of *miR-9-5p* on osteoblast differentiation were also observed in previous studies.

Zheng et al²² found that the expression of *miR-9-5p* was downregulated in human BMSCs (hBMSCs) from osteoporotic patients, and confirmed that *miR-9-5p* inhibits the osteogenic differentiation of hBMSCs. Although our studies did not observe the effects of exosomal *miR-9-5p* on osteoblast apoptosis or proliferation, injection of exosomal *miR-9-5p* into joint cavity clearly ameliorated DMM-induced subchondral bone remodelling, suggesting that *miR-9-5p* might be a hypothetical candidate for the treatment of OA. This may inspire a new approach to develop potential therapeutic agents treating degenerative joints as a whole organ.

Exosomes play an important role in cell-cell communication, which does not need direct cell contact, resulting in a relatively long-distance influence. A growing number of studies are suggesting that exosomes carrying miRNAs are involved in the pathogenesis of OA.²³ Most of these studies focused on the role of exosomes derived from stem cells or synovial fibroblasts in the treatment of OA.^{24,25} Tao et al²⁶ found that exosomes derived from *miR-140-5p* overexpressed human synovial MSCs enhanced cartilage tissue regeneration and prevented OA of the knee in a rat model. However, few studies successfully investigated the role of exosomes from chondrocytes in the pathogenesis of OA. Our study reports for the first time that chondrocyte-derived exosomal *miR-9-5p* could alleviate subchondral bone remodelling through inhibiting osteoblast differentiation in OA.

KLF5 is a transcriptional activator that binds the promoter of target genes or acts downstream of multiple signalling pathways. Previous studies have shown that cartilage matrix degradation is impaired in *KLF5*^{-/-} mice,²⁷ indicating that *KLF* is a critical factor for the maintenance of metabolism of the ECM matrix. In addition, *KLF5* has been confirmed to regulate the Wnt/ β -catenin signalling pathway.²⁸ In the present study, we found that *KLF5* is a functional target gene for *miR-9-5p* mediated matrix metabolism of chondrocytes and osteoblast differentiation.

In conclusion, our data provide new evidence that *circStrn3*-targeting *miR-9-5p/KLF5* is involved in the regulation of cartilage matrix metabolism and subchondral bone remodelling in OA. This study provides a novel understanding of the molecular mechanisms underlying OA, and will hopefully inspire a new approach to developing potential therapeutic agents treating degenerative joints as a whole organ.

Supplementary material



An ARRIVE checklist is included to show that the ARRIVE guidelines were adhered to in this study.

References

1. He CP, Jiang XC, Chen C, et al. The function of lncRNAs in the pathogenesis of osteoarthritis. *Bone Joint Res.* 2021;10(2):122–133.
2. Eglhoff C, Hart DA, Hewitt C, Vavken P, Valderrabano V, Herzog W. Joint instability leads to long-term alterations to knee synovium and osteoarthritis in a rabbit model. *Osteoarthritis Cartilage.* 2016;24(6):1054–1060.
3. Zhong D, Chen XI, Zhang W, Luo Z-P. Excessive tensile strain induced the change in chondrocyte phenotype. *Acta Bioeng Biomech.* 2018;20(2):3–10.
4. Lu J, Zhang H, Cai D, et al. Positive-feedback regulation of subchondral H-type vessel formation by chondrocyte promotes osteoarthritis development in mice. *J Bone Miner Res.* 2018;33(5):909–920.
5. Yu H, Wang X, Cao H. Construction and investigation of a circRNA-associated ceRNA regulatory network in Tetralogy of Fallot. *BMC Cardiovasc Disord.* 2021;21(1):437.
6. Jiao P, Wang X-P, Luoreng Z-M, et al. miR-223: An effective regulator of immune cell differentiation and inflammation. *Int J Biol Sci.* 2021;17(9):2308–2322.
7. Malka Y, Steiman-Shimony A, Rosenthal E, et al. Post-transcriptional 3'-UTR cleavage of mRNA transcripts generates thousands of stable uncapped autonomous RNA fragments. *Nat Commun.* 2017;8(1):2029.
8. Zhang D, Lee H, Zhu Z, Minhas JK, Jin Y. Enrichment of selective miRNAs in exosomes and delivery of exosomal miRNAs in vitro and in vivo. *Am J Physiol Lung Cell Mol Physiol.* 2017;312(1):L110–L121.
9. Shan S-K, Lin X, Li F, et al. Exosomes and bone disease. *CPD.* 2020;25(42):4536–4549.
10. Shao L, Gou Y, Fang J, et al. Parathyroid hormone (1-34) ameliorates cartilage degeneration and subchondral bone deterioration in collagenase-induced osteoarthritis model in mice. *Bone Joint Res.* 2020;9(10):675–688.
11. Shen P, Yang Y, Liu G, et al. CircCDK14 protects against osteoarthritis by sponging miR-125a-5p and promoting the expression of Smad2. *Theranostics.* 2020;10(20):9113–9131.
12. No authors listed. BMKCloud. 2019. <http://en.biocloud.net/> (date last accessed 22 November 2022).
13. Van De Vlekkert D, Qiu X, Annunziata I, d'Azzo A. Isolation, purification and characterization of exosomes from fibroblast cultures of skeletal muscle. *Bio Protoc.* 2020;10(7):e3576.
14. Song T, Ma J, Guo L, Yang P, Zhou X, Ye T. Regulation of chondrocyte functions by transient receptor potential cation channel V6 in osteoarthritis. *J Cell Physiol.* 2017;232(11):3170–3181.
15. No authors listed. TargetScan release 8.0. Whitehead Institute for Biomedical Research. 2021. https://www.targetscan.org/vert_80/ (date last accessed 10 November 2022).
16. Shen S, Wu Y, Chen J, et al. CircSERPINE2 protects against osteoarthritis by targeting miR-1271 and ETS-related gene. *Ann Rheum Dis.* 2019;78(6):826–836.
17. Ling L, Tan Z, Zhang C, et al. CircRNAs in exosomes from high glucose-treated glomerular endothelial cells activate mesangial cells. *Am J Transl Res.* 2019;11(8):4667–4682.
18. Gupta SK, Garg A, Bär C, et al. Quaking inhibits doxorubicin-mediated cardiotoxicity through regulation of cardiac circular RNA expression. *Circ Res.* 2018;122(2):246–254.
19. Kopańska M, Szala D, Czech J, et al. MiRNA expression in the cartilage of patients with osteoarthritis. *J Orthop Surg Res.* 2017;12(1):51.
20. Chen H, Yang J, Tan Z. Upregulation of microRNA-9-5p inhibits apoptosis of chondrocytes through downregulating Tnc in mice with osteoarthritis following tibial plateau fracture. *J Cell Physiol.* 2019;234(12):23326–23336.
21. Jin Z, Ren J, Qi S. Exosomal miR-9-5p secreted by bone marrow-derived mesenchymal stem cells alleviates osteoarthritis by inhibiting syndecan-1. *Cell Tissue Res.* 2020;381(1):99–114.
22. Zheng C, Bai C, Sun Q, et al. Long noncoding RNA XIST regulates osteogenic differentiation of human bone marrow mesenchymal stem cells by targeting miR-9-5p. *Mech Dev.* 2020;162:103612.
23. Asghar S, Litherland GJ, Lockhart JC, Goodyear CS, Crilly A. Exosomes in intercellular communication and implications for osteoarthritis. *Rheumatology (Oxford).* 2020;59(1):57–68.
24. Mianehsaz E, Mirzaei HR, Mahjoubin-Tehran M, et al. Mesenchymal stem cell-derived exosomes: a new therapeutic approach to osteoarthritis? *Stem Cell Res Ther.* 2019;10(1):340.
25. Liu Y, Lin L, Zou R, Wen C, Wang Z, Lin F. MSC-derived exosomes promote proliferation and inhibit apoptosis of chondrocytes via lncRNA-KLF3-AS1/miR-206/GIT1 axis in osteoarthritis. *Cell Cycle.* 2018;17(21–22):2411–2422.
26. Tao S-C, Yuan T, Zhang Y-L, Yin W-J, Guo S-C, Zhang C-Q. Exosomes derived from miR-140-5p-overexpressing human synovial mesenchymal stem cells enhance cartilage tissue regeneration and prevent osteoarthritis of the knee in a rat model. *Theranostics.* 2017;7(1):180–195.
27. Shinoda Y, Ogata N, Higashikawa A, et al. Kruppel-like factor 5 causes cartilage degradation through transactivation of matrix metalloproteinase 9. *J Biol Chem.* 2008;283(36):24682–24689.
28. Zhang X, Lou Y, Zheng X, et al. Wnt blockers inhibit the proliferation of lung cancer stem cells. *Drug Des Devel Ther.* 2015;9:2399–2407.

Author information:

- B. Li, MD, Postgraduate
 - T. Ding, MD, Postgraduate
 - H. Chen, MD, Postgraduate
 - C. Li, PhD, Research Fellow
 - B. Chen, PhD, Research Fellow
 - X. Xu, MD, Research Fellow
 - P. Huang, BSc, Research Fellow
 - F. Hu, BSc, Research Fellow
 - L. Guo, PhD, Research Fellow
- Department of Orthopaedics, Shanghai Key Laboratory for Prevention and Treatment of Bone and Joint Diseases, Shanghai Institute of Traumatology and Orthopaedics, Ruijin Hospital, Shanghai Jiao Tong University School of Medicine, Shanghai, China.

Author contributions:

- B. Li: Conceptualization, Writing – original draft.
- T. Ding: Formal Analysis, Writing – review & editing.
- H. Chen: Formal Analysis, Writing – review & editing.
- C. Li: Investigation, Formal Analysis.
- B. Chen: Software, Data curation.
- X. Xu: Data curation, Methodology.
- P. Huang: Software.
- F. Hu: Methodology, Writing – review & editing.
- L. Guo: Conceptualization, Writing – original draft, Writing – review & editing.

- B. Li and T. Ding contributed equally to this work.

- F. Hu and L. Guo contributed equally to this work.

Funding statement:

- The authors disclose receipt of the following financial or material support for the research, authorship, and/or publication of this article: funding from The National Science Foundation of China (No. 81870617, 81803242), Shanghai Talent Development Funding Scheme (No. 2019046), and The Science and Technology Commission of Shanghai Municipality (No. 15411950900).

Acknowledgements:

- The authors wish to thank the technical service support and venue support of Department of Orthopaedics, Shanghai Key Laboratory for Prevention and Treatment of Bone and Joint Diseases.

Ethical review statement:

- All animal experiments were performed according to the protocol approved by the Shanghai Jiao Tong University (SJTU) Animal Care and Use Committee.

© 2023 Author(s) et al. This is an open-access article distributed under the terms of the Creative Commons Attribution Non-Commercial No Derivatives (CC BY-NC-ND 4.0) licence, which permits the copying and redistribution of the work only, and provided the original author and source are credited. See <https://creativecommons.org/licenses/by-nc-nd/4.0/>